

Raman Scattering by Coupled-Layer Plasmons and In-Plane Two-Dimensional Single-Particle Excitations in Multi-Quantum-Well Structures

G. Fasol, N. Mestres, H. P. Hughes,^(a) A. Fischer, and K. Ploog

Max-Planck-Institut für Festkörperforschung, D-7000 Stuttgart 80, Federal Republic of Germany

(Received 18 September 1985)

Raman measurements are reported of collective modes (plasmons) and single-particle excitations in modulation-doped GaAs/Al_xGa_{1-x}As quantum-well systems as a function of the wave-vector component k_{\parallel} parallel to the electron layers. Samples with five layers show discrete layer-plasmon modes manifesting the coupling of the electrons in different layers by Coulomb interaction. The Raman spectra due to single-particle excitations are narrow bands peaking at $\hbar k_{\parallel} v_F^{2D}$ characteristic for the response of a 2D electron gas.

PACS numbers: 78.30.Gt, 71.45.Gm, 73.40.Lq

In the present paper we report Raman measurements of the single-particle intraband excitation spectra (SPE) and the collective intraband modes (plasmons) for finite-layered electron-gas systems and their dependence on the wave-vector component k_{\parallel} parallel to the layers. The collective intraband modes are the discrete coupled-layer plasmons predicted by Jain and Allen.¹ The selection rules are the same as for bulk GaAs. We discuss the relevance of surface-plasmon modes predicted by Giuliani and Quinn² for the present experiments.

The dielectric response (in particular, the plasmon excitations) of the two-dimensional electron gas (2DEG)³⁻⁵ and of the layered 2DEG⁶⁻⁹ with an infinite or semi-infinite number of layers has been studied in great detail theoretically. While there is a large amount of spectroscopic information on intersubband excitations of the 2DEG there are far fewer experiments on intraband excitation probing the 2DEG and coupled 2DEG's along the directions in which the electrons are free. Collective excitations (plasmons) in single 2DEG have been studied thoroughly with use of grating coupler techniques¹⁰ and there are two reports on single Raman signals from an intraband plasmon.^{11,12}

The plasmon frequency ω_p^{2D} is proportional to $k_{\parallel}^{1/2}$ in a single 2DEG.^{3,4} In a layered electron gas the plasma resonance frequencies ω_p fan out into a band because of the Coulomb interaction between the layers. The motion of electrons in the different layers becomes correlated and there are N eigenmodes in a system of N charge layers.¹ The N eigenmodes may be assigned parameters $k_{\perp}(n) = 2\pi n/Nd$, where $n = 1, \dots, N$ and d is the separation of layers. $k_{\perp}(n)$ describes the phase relationship between layers for the plasmon mode n , but loses its physical meaning as a wave vector for small N . In the present work we observe these discrete plasmon modes, a manifestation of the correlation of electronic motion in different layers.

The second main result of the present work is our Raman measurements of the SPE spectra as functions

of k_{\parallel} obtained in crossed polarization. To the best of our knowledge there has been no previous experimental report of single-particle intraband excitations either of a single 2DEG or a layered electron gas. The Raman spectra in this case are directly proportional to the imaginary part of the dielectric polarizability of the 2DEG, $\text{Im}[\chi(k_{\parallel}, \omega)]$ [see Eq. (2.92) of the work of Abstreiter, Cardona, and Pinczuk¹³]. They show the characteristic narrow shape of the single-particle spectrum in two dimensions as predicted in Ref. 5. This is very different from the behavior of the three-dimensional electron gas, where the SPE spectrum has a triangular shape.

We measured several modulation-doped multi-quantum-well GaAs/Al_xGa_{1-x}As systems in which the conduction-band electrons form a layered electron gas with a finite number of layers. Results for sample No. 4849 are presented in this paper. It consists of five periods. Each period comprises a 500-Å-wide GaAs quantum well surrounded by a 50-Å AlAs buffer layer on one side, a 100-Å Al₃₀Ga₇₀As buffer layer on the other side. A 250-Å Si-doped Al₃₀Ga₇₀As layer was grown between the buffer layers of subsequent wells, with a doping concentration of $n \approx 2 \times 10^{18} \text{ cm}^{-3}$. The sample structure is shown schematically in the inset of Fig. 2. The structures have very high mobilities (up to $4 \times 10^5 \text{ cm}^2/\text{V} \cdot \text{s}$) presumably due to the deliberate asymmetric structure of the well. Carrier densities of all samples have been determined from Hall-effect measurements at 5 K under saturating illumination and, in addition, for the case of two samples including No. 4849 by Shubnikov-de Haas (SdH) measurements at 1.25 K. Up to thirty oscillations of ρ_{xx} could be observed. Apart from spin splitting at high magnetic fields no evidence of oscillations other than the main period was found. This shows that *only a single sheet* of electrons per well contributes. A significant contribution from a higher subband or a second sheet of charge per well would appear as a second period of oscillation in the SdH measurements.¹⁴ Surface band bending due to surface defects should be confined to the surface layer, 250 Å of which are high-

ly ($2 \times 10^{18} \text{ cm}^{-3}$) *n*-doped $\text{Al}_{30}\text{Ga}_{70}\text{As}$. The carrier density of sample No. 4849, for which the results are reported here, is $6.8 \times 10^{11} \text{ cm}^{-2}$. The Hall mobility under the same conditions mentioned above is $1.8 \times 10^5 \text{ cm}^2/\text{V} \cdot \text{s}$.

The resonant Raman measurements were performed slightly above the fundamental gap at a sample temperature of 10 K with use of a LD700 dye laser operating between 7700 and 8040 Å pumped by a 4-W Kr^+ laser. The scattering geometry is shown in the inset of Fig. 1. For the angle between incident and collected light values between 6° and 10° were chosen. Rotating

the sample by a controlled amount between experiments allowed us to study the dependence on wave-vector transfer parallel to the sample layers, $q_{\parallel, \text{sample}}$ between zero and a little less than twice the wave-vector of the laser photon $q_{\perp, \text{vacuum}}$. The wave-vector transfer Δq_{\perp} perpendicular to the sample is essentially constant because of the large refractive index $n \approx 3.6$ of the structure. It is $\Delta q_{\perp} = 5.6 \times 10^5 \text{ cm}^{-1}$ for the laser energy used here.

Figure 1 shows the Raman spectra of the low-lying electronic excitations and their dependence on k_{\parallel} for incident and collected light polarized both parallel [Fig. 1(a)] and perpendicular [Fig. 1(b)] to each other for one of the samples with five layers (No. 4849). The spectra of Fig. 1(a) are interpreted as collective modes. The spectral peaks labeled 1 to 5 are assigned to the coupled-layer modes predicted by Jain and Allen.¹ These spectral features only appear in parallel polarization.

The Raman spectra for crossed polarization are shown in Fig. 1(b). They peak at frequencies very close to $\hbar k_{\parallel} v_F^{2D}$. v_F^{2D} is the 2D Fermi velocity, which we determined using the electron density from Hall and SdH measurements. Using the usual selection rules,¹³ we assign these Raman signals to spin-density excitations associated with the motion parallel to the layers. The Raman intensity due to spin-density excitations is directly proportional to the imaginary part of the polarizability, $\text{Im}[\chi(k_{\parallel}, \omega)]$.¹³ The results of a simplifying calculation of the Raman line shapes using the full Eq. (2.92) of Ref. 13 and using $\text{Im}[\chi(k_{\parallel}, \omega)]$ from Ref. 5 are shown as the dotted lines in Fig. 1(b). Since the carrier density is determined by Hall and SdH experiments there is no free parameter. The agreement is good. The measured spectra are somewhat wider than the calculated shapes, since the relaxation time is neglected in the present calculations. The spectra are proportional to the density of single-particle excitations associated with the motion parallel to the layers of the sample. In 2D the density of SPE is narrow and shows a peak at $\hbar k_{\parallel} v_F^{2D}$ as opposed to the triangle-like shape in 3D. Since the spin-density excitations are not accompanied by charge-density fluctuations, the coupling between layers by the Coulomb interaction is not relevant, contrary to the case of the layer plasmons. Therefore k_{\perp} dependence is expected to be weak.

For two samples (including sample No. 4849) we have measured the resonance profile of the single-particle spectrum. We could only measure above 1.56 eV, since the background luminescence is too strong at lower energies. The Raman cross section decreases with increasing energy above 1.56 eV and drops to a very small value within around 40 meV. Comparing these results with luminescence excitation spectra of the same samples we conclude that the single-particle

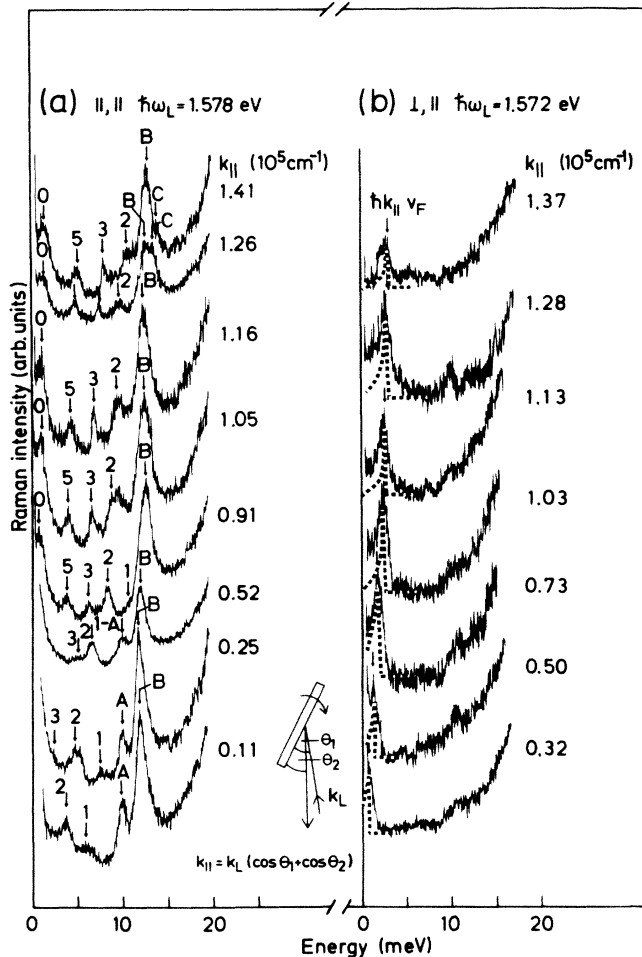


FIG. 1. Raman spectra of modulation-doped multiheterojunction structure with five periods. The Raman intensity is plotted as a function of the energy shift measured from the laser. k_{\parallel} denotes the wave-vector component parallel to the layers. ($T=10 \text{ K}$, laser power density was around $40 \text{ mW}/\text{cm}^2$; for sample parameters see text.) Inset: The scattering geometry. (a) Polarized spectra (\parallel, \parallel) showing collective modes (plasmons) of layered electron gas. (b) Crossed polarization (\parallel, \perp) showing single-particle excitation spectra. Dotted lines show simplifying calculation for the line shapes using Eq. (2.92) from Ref. 13 and $\text{Im}[\chi^{2D}(k_{\parallel}, \omega)]$ from Ref. 5.

scattering is a two-step process¹³ involving the lowest electron quantum-well level and the lowest and higher hole quantum-well levels.

Figure 2 shows the energies of the Raman peaks of sample No. 4849 as a function of the in-plane wave vector k_{\parallel} . Shown in Fig. 2 as solid lines are calculations of the plasmon dispersion of a system of five infinitely thin layers of electrons. We use the method of Ref. 1, taking account of the dielectrically relevant cover layer of 400 Å to calculate the coupled-layer plasmons. This calculation is not a fit since there are no adjustable parameters. For our purpose we found it numerically more stable to diagonalize Eq. (5) of Ref. 1. Three of the calculated modes ($n=1, 2$, and 3) fall very close to the measured plasmon modes. The theoretical dispersion for the lowest layer mode ($n=5$) deviates somewhat from the measured values. This deviation might be due to the fact that the calculation assumes infinitely thin electron layers, while in realistic samples the electrons have considerable spatial extent perpendicular to the wells. The calculated

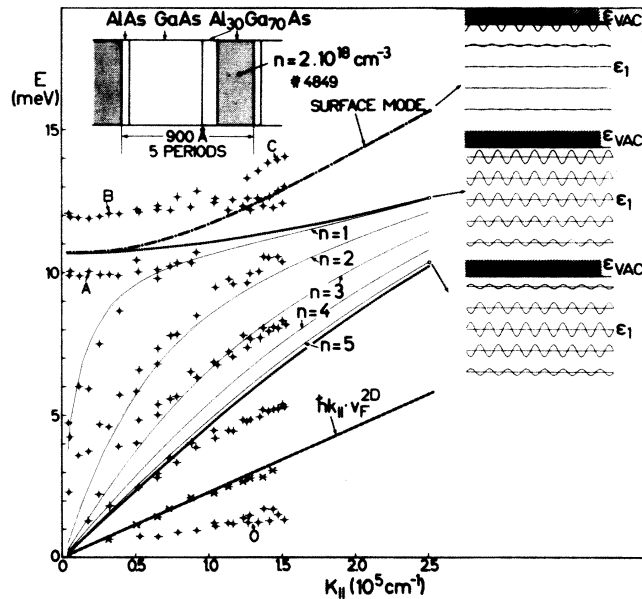


FIG. 2. Energy of Raman peaks as a function of wave-vector component k_{\parallel} parallel to the layers for sample No. 4849 (five layers). Solid lines show the results of a calculation using the methods of Ref. 1. Only known sample parameters are used for the calculation. Dotted line shows the limits of the layer-plasmon band for a system with an infinite number of layers. Dash-dotted line shows calculated surface mode for semi-infinite system without dielectric surface cover layer and otherwise similar parameters as sample No. 4849. Crosses show position of single-particle excitation peaks. Dashed line shows $\hbar k_{\parallel} v_F^{2D}$, where v_F^{2D} is calculated from the carrier density known from Hall and Shubnikov-de Haas experiments. On the right-hand side the charge-density oscillations for three eigenmodes are shown (see text).

mode for $n=4$ does not correspond to a measured mode. We could not improve the overall agreement of the theoretical dispersion curves with the experimental data by changing the density of carriers per layer, nor by assuming that the top layer is empty as a result of the surface depletion layer (which we believe is not the case for the present structure). Our measurements, therefore, clearly show that the theory has to be extended to include the finite width of the wave functions in order to explain the plasmon dispersion of realistic samples.

The crosses mark the measured values for the peaks of the single-particle excitation spectra discussed above. They are well explained by $\hbar k_{\parallel} v_F^{2D}$ (dashed line). Since v_F^{2D} is fully determined by the density of electrons, the dashed line is independently determined and not a fit to the data.

We have so far shown that we have observed the single-particle excitation spectra [Fig. 1(b)] and the coupled-layer plasmon modes [peaks 1 to 5 in Fig. 1(a)] in multiple-quantum-well samples with a small number of layers. In addition to the above-mentioned Raman signals the spectra contain further Raman peaks in the spectral region studied here [0, A, B, C in Fig. 1(a) and a weak peak near 10 meV in Fig. 1(b)]. These features are not crucial to the argumentation of the present work. Nevertheless we insert a section on their interpretation at this point.

There are two modes, near 9.9 meV (labeled A) and near 12.0 meV (labeled B). They appear also in spectra measured with $k_{\parallel}=0$. Mode A and mode B increase weakly with increasing k_{\parallel} . For k_{\parallel} values larger than $1.0 \times 10^5 \text{ cm}^{-1}$ a satellite C appears above mode B. C also increases with increasing k_{\parallel} . We interpret these modes to be mixed modes¹⁵ of collective intersubband modes I_{-} (coupled with LO phonons¹²) and the in-plane plasmon modes. The present interpretation is consistent with the fact that in all sample structures we saw a weak Raman signal due to the spin-flip excitations in crossed polarization near 10 meV [Fig. 1(b)]. For an unambiguous identification of signals A, B, and C with mixed intersubband and intrasubband collective modes we are at present conducting self-consistent subband structure calculations. We will combine these with our Raman and luminescence excitation measurements to obtain the subband structure. We note that mode I_{-} of Ref. 12 decreases with increasing k_{\parallel} for small k_{\parallel} contrary to the behavior of our mode C.

We consider an alternative explanation invoking coupled intersubband and surface plasmon¹⁶ modes or identifying mode C as an intersubband surface mode¹⁷ as far less likely at this stage. Indeed, contrary to the behavior of mode C in our measurements, the intersubband surface mode is predicted to decrease in energy with increasing k_{\parallel} .¹⁷ A third possible interpretation would be a surface plasmon mode, which would

replace mode $n=1$ in the region of high k_{\parallel} and lie between the "ideal" surface mode (for the case of a semi-infinite number of layers) shown as the dash-dotted line and the upper limit of the plasmon band limits (dotted lines) in Fig. 2. However, since the dielectrically relevant thickness of the surface layer in our structures is around 400 Å the condition $d_{\text{surf}} < d/2$ will, if at all, only be just fulfilled. Therefore a surface mode, if existent, would only deviate insignificantly from mode $n=1$ in the "bulk" case.

The lowest mode (labeled 0) in Fig. 2 depends approximately linearly on k_{\parallel} . The assignment of this mode is not yet clear. This mode lies in a region where collective modes should be Landau damped by the coupling to single-particle excitations. However, since the single-particle excitation density in 2D shows a narrow peak near $\hbar k_{\parallel} v_F^{2D}$, as we measured [Fig. 1(b)], the Landau damping of mode 0 may well be expected to be weak, since it falls into a region of low density of single-particle excitations. This is a behavior uncommon for 3D systems.

To demonstrate the physical character of the layer plasmon modes we show three of the modes schematically as an inset on the right-hand side of Fig. 2. We calculate these results from the eigenvectors obtained from Eq. (5) of Ref. 1. For each mode we plot the deviation from the equilibrium density of electrons as a function of the space coordinate parallel to the layers for all five layers. The highest-energy mode is a surface-plasmon mode, calculated here for a fictitious five-layer structure with the parameters of sample No. 4849 but without the dielectric surface layer. The other two modes shown are the $n=1$ and the $n=5$ plasmon eigenmodes of sample No. 4849. As expected, the charges oscillate in phase for the mode with highest energy, and avoid each other as much as possible for the mode with lowest energy.

The plasmon modes shown in Fig. 1(a) have widths between 0.5 and 1.0 meV. This agrees well with the widths calculated by Jain and Allen,¹⁸ which are caused by the momentum broadening due to the finite penetration depth of the light.

In conclusion, we have reported Raman measurements of the discrete layer plasmons and of the single-particle excitation spectra in the layered electron gas of multi-quantum-well structures. Because of the Coulomb interaction between electrons on different

layers the motion of electrons on different layers becomes correlated. Therefore, each of the N discrete layer-plasmon modes of a sample with N layers has a different dependence of its frequency on k_{\parallel} . The Raman spectra in crossed polarization are proportional to the single-particle excitations associated with the motion of electrons parallel to the layers. They show narrow bands peaking at $\hbar k_{\parallel} v_F^{2D}$, typical for the single-particle excitations in two dimensions.

We express our deep gratitude to Professor M. Cardona for his help and support, to M. Dobers for the SdH measurements, and to H. Hirt, M. Siemers, and P. Wurster for technical assistance. One of us (G.F.) expresses his gratitude to Dr. G. Lonzarich for numerous helpful discussions.

^(a)On leave from Cavendish Laboratory, Madingley Road, Cambridge CB3 0HE, England.

¹J. K. Jain and P. B. Allen, Phys. Rev. Lett. **54**, 2437 (1985).

²G. F. Giuliani and J. J. Quinn, Phys. Rev. Lett. **51**, 919 (1983).

³R. H. Ritchie, Phys. Rev. **106**, 874 (1957).

⁴R. A. Ferrell, Phys. Rev. **111**, 1214 (1958).

⁵F. Stern, Phys. Rev. Lett. **18**, 546 (1967).

⁶A. L. Fetter, Ann. Phys. (N.Y.) **81**, 367 (1973).

⁷A. L. Fetter, Ann. Phys. (N.Y.) **88**, 1 (1974).

⁸D. Greco, Phys. Rev. B **8**, 1958 (1973); J. K. Jain and P. B. Allen, Phys. Rev. B **32**, 997 (1985).

⁹S. Das Sarma and J. J. Quinn, Phys. Rev. B **25**, 7603 (1982).

¹⁰For a recent review see D. Heitmann, Surf. Sci. (to be published).

¹¹D. Olego, A. Pinczuk, A. C. Gossard, and W. Wiegmann, Phys. Rev. B **25**, 7867 (1982).

¹²R. Sooryakumar, A. Pinczuk, A. C. Gossard, and W. Wiegmann, Phys. Rev. B **31**, 2578 (1985).

¹³G. Abstreiter, M. Cardona, and A. Pinczuk, in *Light Scattering in Solids IV*, edited by M. Cardona and G. Güntherodt (Springer-Verlag, Heidelberg, 1984), p. 5.

¹⁴A. Kastalsky, R. Dingle, K. Y. Cheng, and A. Y. Cho, Appl. Phys. Lett. **41**, 274 (1982).

¹⁵Sankar Das Sarma, Phys. Rev. B **29**, 2334 (1984).

¹⁶J. K. Jain, Phys. Rev. B **32**, 5456 (1985).

¹⁷P. Hawrylak, Ji-Wei Wu, and J. J. Quinn, Phys. Rev. B **32**, 5169 (1985).

¹⁸J. K. Jain and P. B. Allen, Phys. Rev. Lett. **54**, 947 (1985).

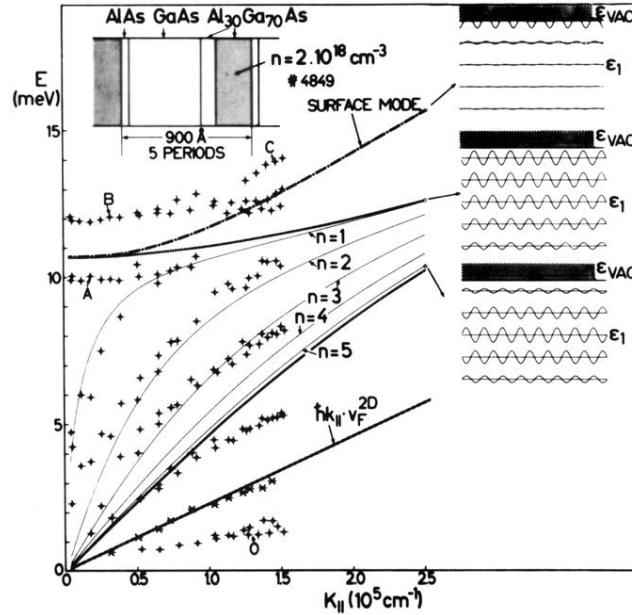


FIG. 2. Energy of Raman peaks as a function of wave-vector component $k_{||}$ parallel to the layers for sample No. 4849 (five layers). Solid lines show the results of a calculation using the methods of Ref. 1. Only known sample parameters are used for the calculation. Dotted line shows the limits of the layer-plasmon band for a system with an infinite number of layers. Dash-dotted line shows calculated surface mode for semi-infinite system without dielectric surface cover layer and otherwise similar parameters as sample No. 4849. Crosses show position of single-particle excitation peaks. Dashed line shows $\hbar k_{||} v_F^{2D}$, where v_F^{2D} is calculated from the carrier density known from Hall and Shubnikov-de Haas experiments. On the right-hand side the charge-density oscillations for three eigenmodes are shown (see text).